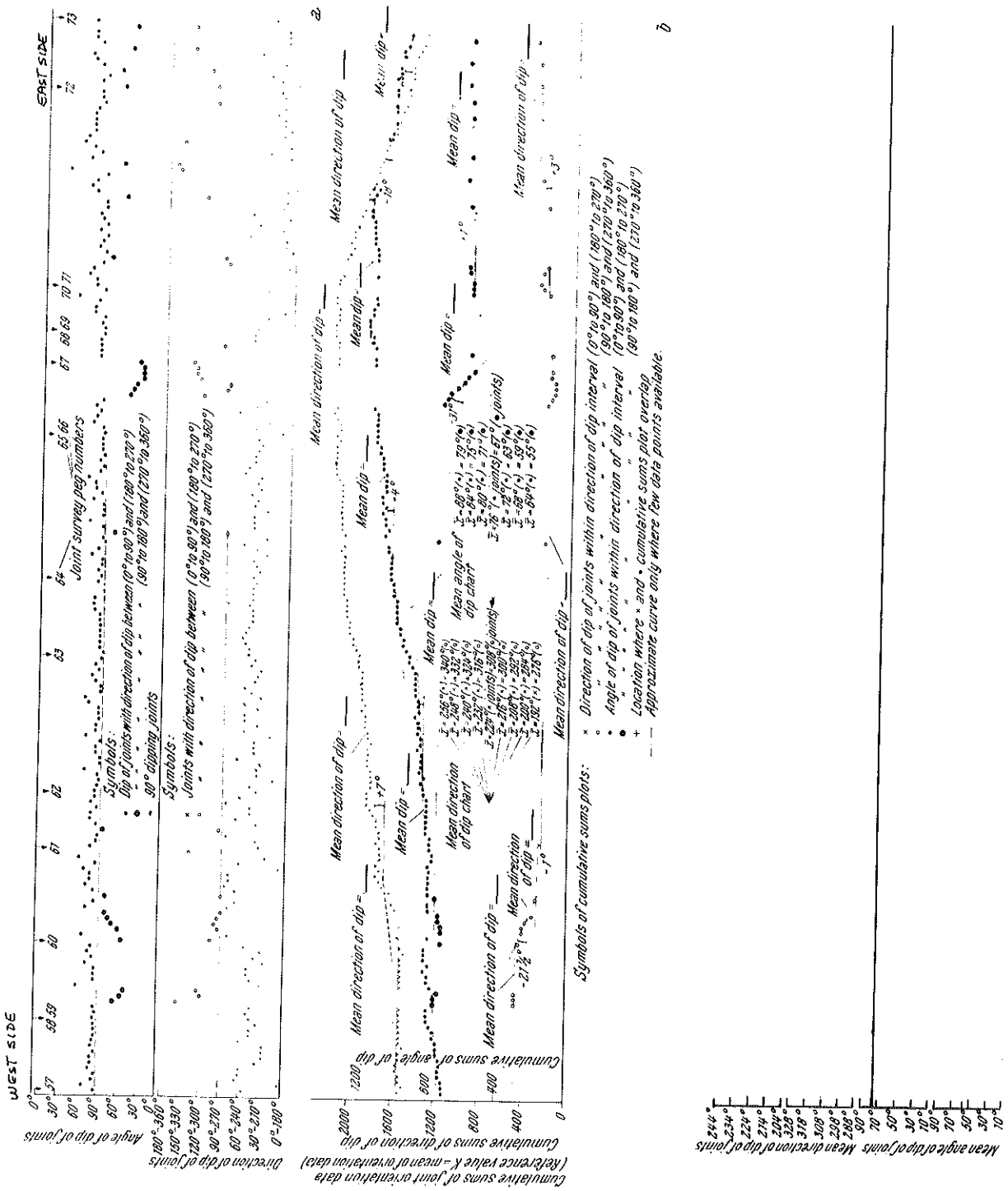

Fig. 16 Example of cumulative sums technique for analyzing two sets of joint data showing (a) the raw dip data and (b) cumulative sums plots of the data for both dip and direction of the dip.

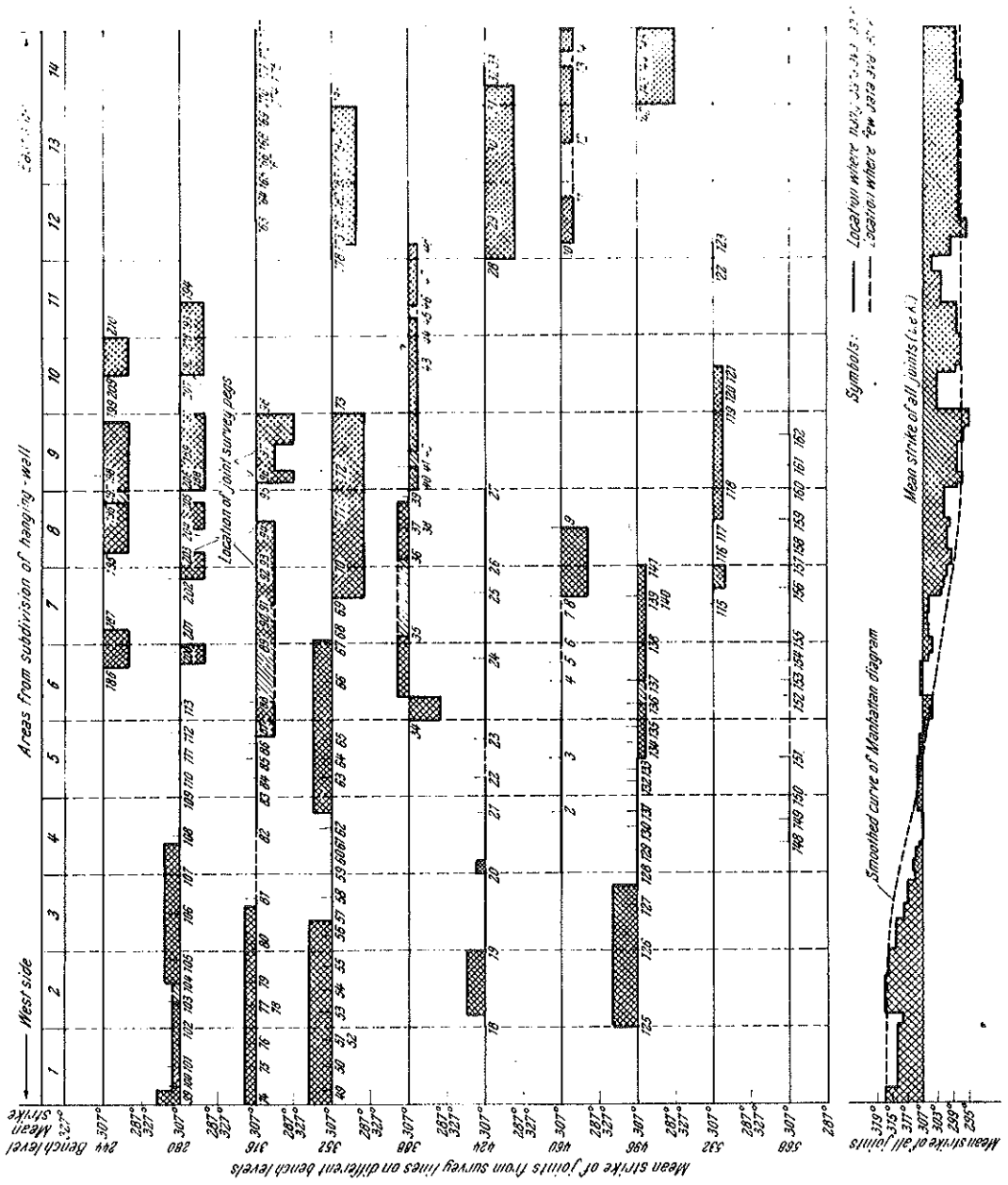

Fig. 17 Manhattan diagrams for different benches of cumulative sums results of strike values of a dominant joint set on a high wall in argillite. Note the average values for all benches at the bottom of the figure.

2. SOLUTIONS TO QUESTIONS ON DEFINING JOINT SETS AND RELATED CHARACTERISTICS

(a) *Problem 1*

(i) The plotted poles and planes are shown in Fig. 1(S)

(ii) The geometric relationships of the planes in Fig. 1(S) are as follows:

- The angle (δ) between the poles of Plane A and B (γ) is as follows:
  $\delta = 76^{\circ}$
- The angle between the planes is
  $W = 180 - \delta = 180 - 76 = 104^{\circ}$
- The bearing and plunge of the line of intersection are on Fig. 1(S) as $044/20^{\circ}$.
- The apparent dip of Plane A in Plane B is the plunge of the line of intersection = 20°.
- The pitch (β) of Plane A in Plane B is measured along the great circle of Plane B to be 67° as shown in Fig. 1(S)

(b) *Problem 2*

The completed point count for the scatter diagram is shown in Fig. 2(S) and the contoured diagram is shown in Fig. 3(S) The orientation and density characteristics of the main joint sets are as follows:

Set	Strike	Dip	No. of Poles at Peak	% of Total at Peak
1	020	27E	7	14
2	001	78W	9	18
3	090	89S	7	14

(c) *Problem 3*

The contoured diagrams for these printouts are shown in Figs. 4(S) (a and b), 5(S) (a and b), 7(S) and 8(S). The orientation and percent concentration of the joint sets are as follows:

Figure	Joint Set	Strike	Dip	Percent Concentration at Peak
4(S) (a and b)	A	78	72N	19
	B	78	78S	8
	C	163	80W	5
5(S) (a and b)	Bedding	45	26SE	35
7(S)	Foliation	94	46N	18
8(S)	Joint Set C	130	25SW	28

(d) *Problem 4*

(a) The profiles of the joint sets are shown in Fig. 9(S) The probability of obtaining a joint of Joint Set A with a dip of 60° is determined from the profile to be:

$$P_{60} = \frac{A_{60}}{A_T} = \frac{1.01}{6.26} = .16 = 16\%$$

(b) The contoured printouts in Fig. 10(S) and 11(S) indicate that these joint sets fit the spherical normal distribution relatively well. Fig. 12(S) shows the contoured plots for the two joint sets discussed above as well as additional joint sets in the same rock type. It can be seen that Joint Sets A and C are relatively uniform, whereas Joint Sets B and D are somewhat skewed.

(e) *Problem 5*

(i) The relative frequency of joints in Fig. 12 with joint lengths of 5 ft and 10 ft is 10.11% and 4.52%, respectively. The percentage of joints greater than 5 ft and 10 ft in length is 24.39% (i.e. 100.0 - 75.61) and 7.32% (i.e. 100.0 - 92.86), respectively.

(ii) The frequency distribution of dip continuity of joints with no ends out, as shown in a typical histogram in Fig. 12, follows a log-normal distribution. That is, the natural logarithm of joint size is normally distributed, or that the function $\frac{\ln x - \mu}{\sigma}$ is distributed as the standard normal, where x = joint size; μ = mean of $\ln$, and σ = standard deviation of $\ln$ The μ and σ values were estimated using log-normal probability paper to be 3.367 and 0.884, respectively. It should be noted that although the distribution in Fig. 12 for argillite rocks was found to fit a log-normal distribution, for joints in amygdaloidal lava at DeBeers Mine in South Africa the frequency distribution of dip continuity was found to fit an exponential function of the form

$$y = e^{-\alpha x}.$$

It is of interest to note that the majority of joints within a set, such as shown in Fig. 12, are very small, the mean length of the joints being only 4.74 ft.

(f) *Problem 6*

(i) The percentage of joints softer than hardness R2 in Fig. 13 is 71.77%.

(ii) If the mean hardness is 6.89 based on the system established in Fig. 13, the rock hardness classification for this value is between R1 and R2, being $\frac{0.89}{1.00}$(R1) = (0.89) R1. The minimum mean unconfined compressive strength for the rock according to the strength envelope in Fig. 14 for (0.89)(R1) is 700 psi.

(g) *Problem 7*

(i) The current mean direction of dip and the respective Manhattan diagrams from the cusums curves in Fig. 15(b) are given in Fig. 13(S).

(ii) Both the current mean dip and mean direction of dip of the cusums plots of both sets of joint data in Fig. 16 are given in Fig. 14(S). Also, given in Fig. 14(S) are the four respective Manhattan diagrams for these cusums curves.

(iii) In Fig. 17 it can be seen that the mean strike of all the joints is 307^{o} (i.e. K = 307^{o}). There is, however, a counter-clockwise rotation in the current mean strike, going from west to the east side of the slope. The mean strike rotates from about 317^{o} in areas 1 and 2 (areas of the slope determined by arbitrary vertical limits for convenience) to about 297^{o} in areas 9 to 14. Around areas 5 and 6 the current mean strike is about the same as K (i.e. 307^{o}). The rate of change of this rotation is greatest in areas 3 to 7. This rotation is due to a major fault, the only major fault occurring in the area considered. This fault strikes 320^{o} and dips 80^{o} to 85^{o} SW, indicating that these joints are probably feather fractures which have developed sympathetic to the fault. Sympathetic fracturing parallel to the fault has swung the current mean strike slightly towards that of the fault. Further east, however, the southwest dipping joints rotate counter-clockwise past the mean. Beyond area 9, where the influence of the fault is negligible, and where only tectonic forces appear to have been significant in causing the existing joints, the joints maintain a remarkably consistent current mean strike of about 295^{o}. In terms of extrapolation to the east the results in Fig. 17 indicate that the current mean strike is, statistically speaking, remarkably consistent east of area 8. The deviation about the mean strike is generally less than $\pm 3^{o}$. In that these features are regional joint structure, there is good evidence, and hence good reason to believe, that the strike of these joints will be reasonably similar in areas further east.

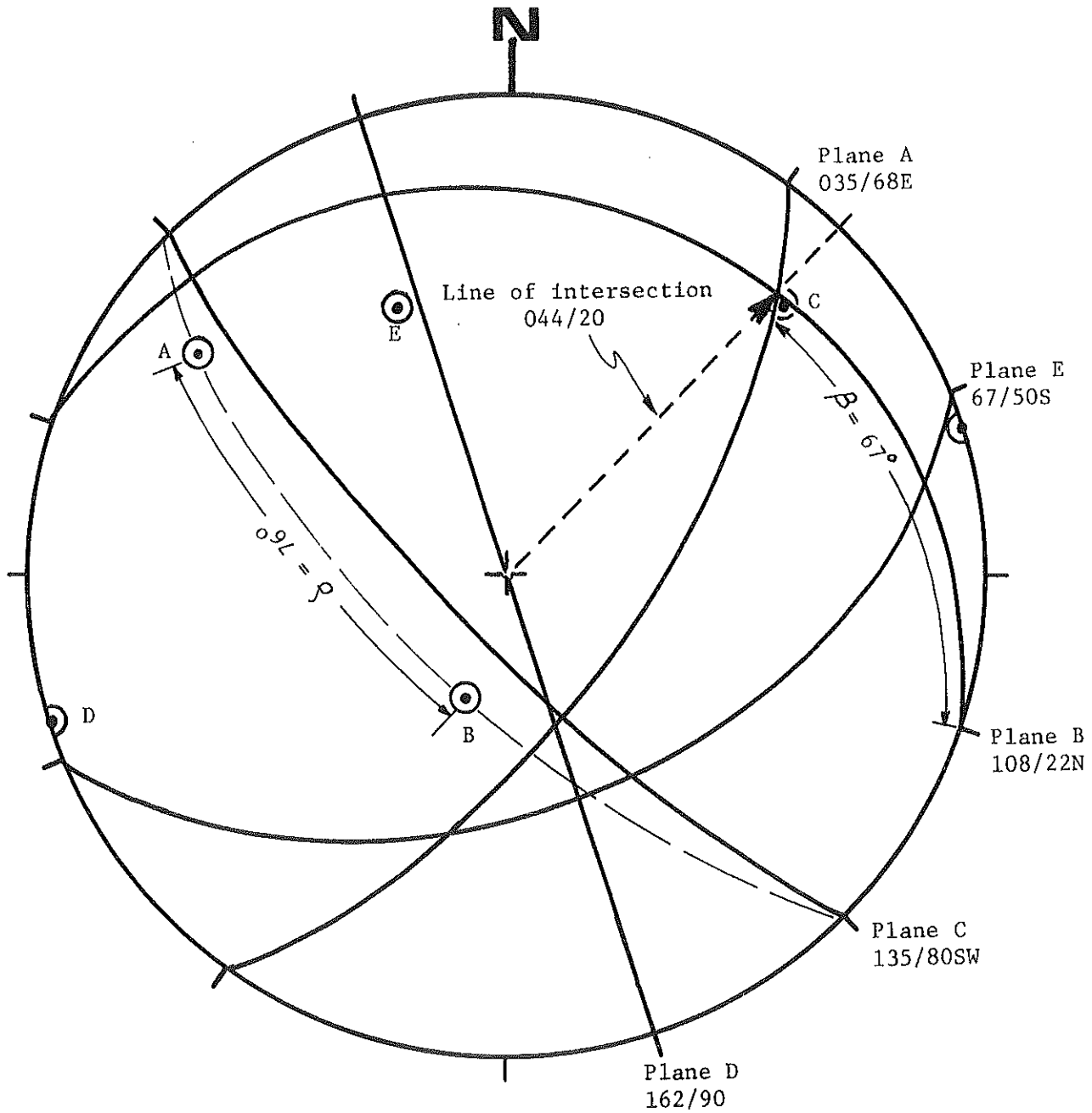

Fig. 1 (S) Equal area plot of poles and planes of joints.

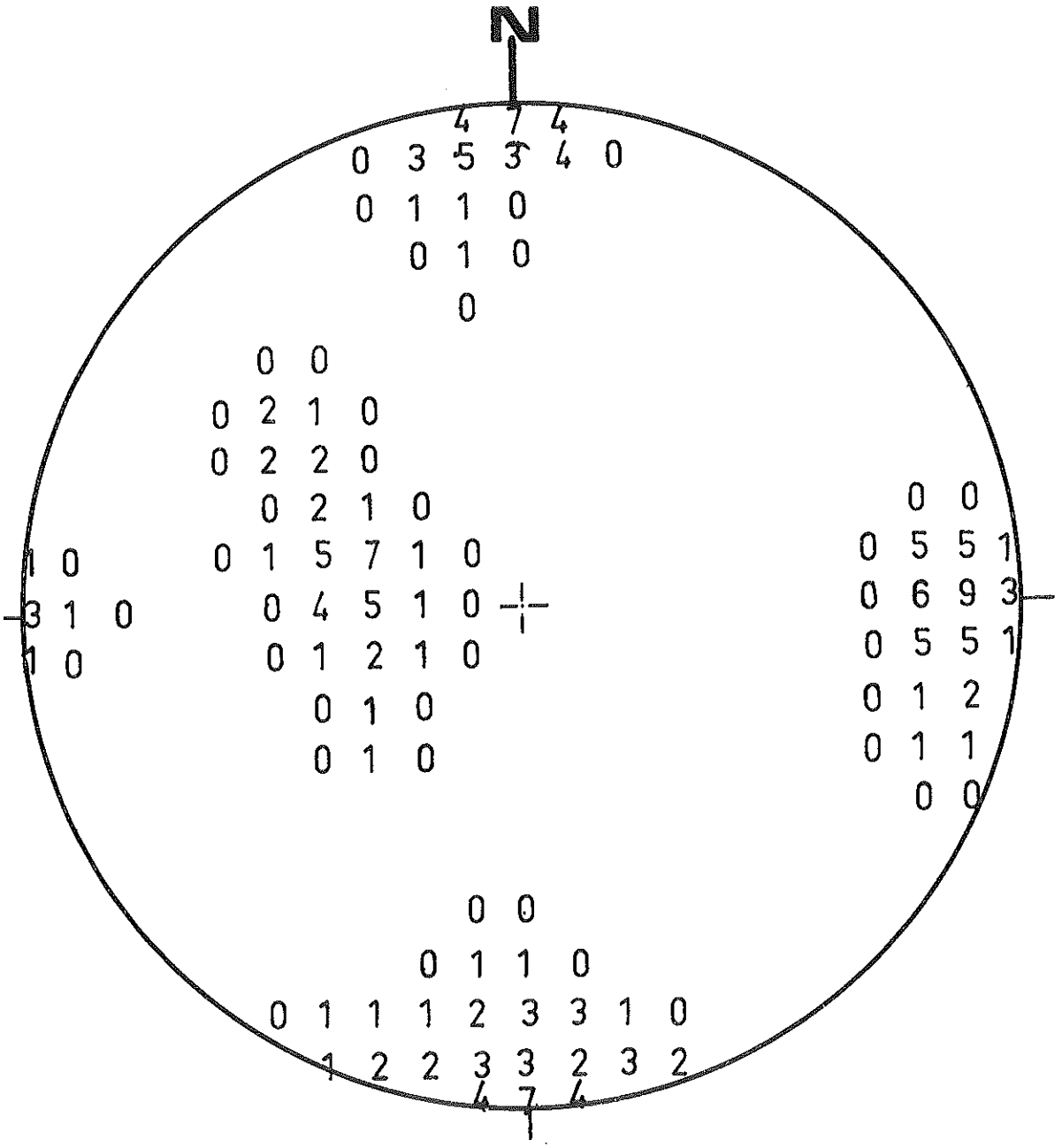

Fig. 2 (S) Point contact diagram of equal area plot of poles to joint planes in a rock mass.

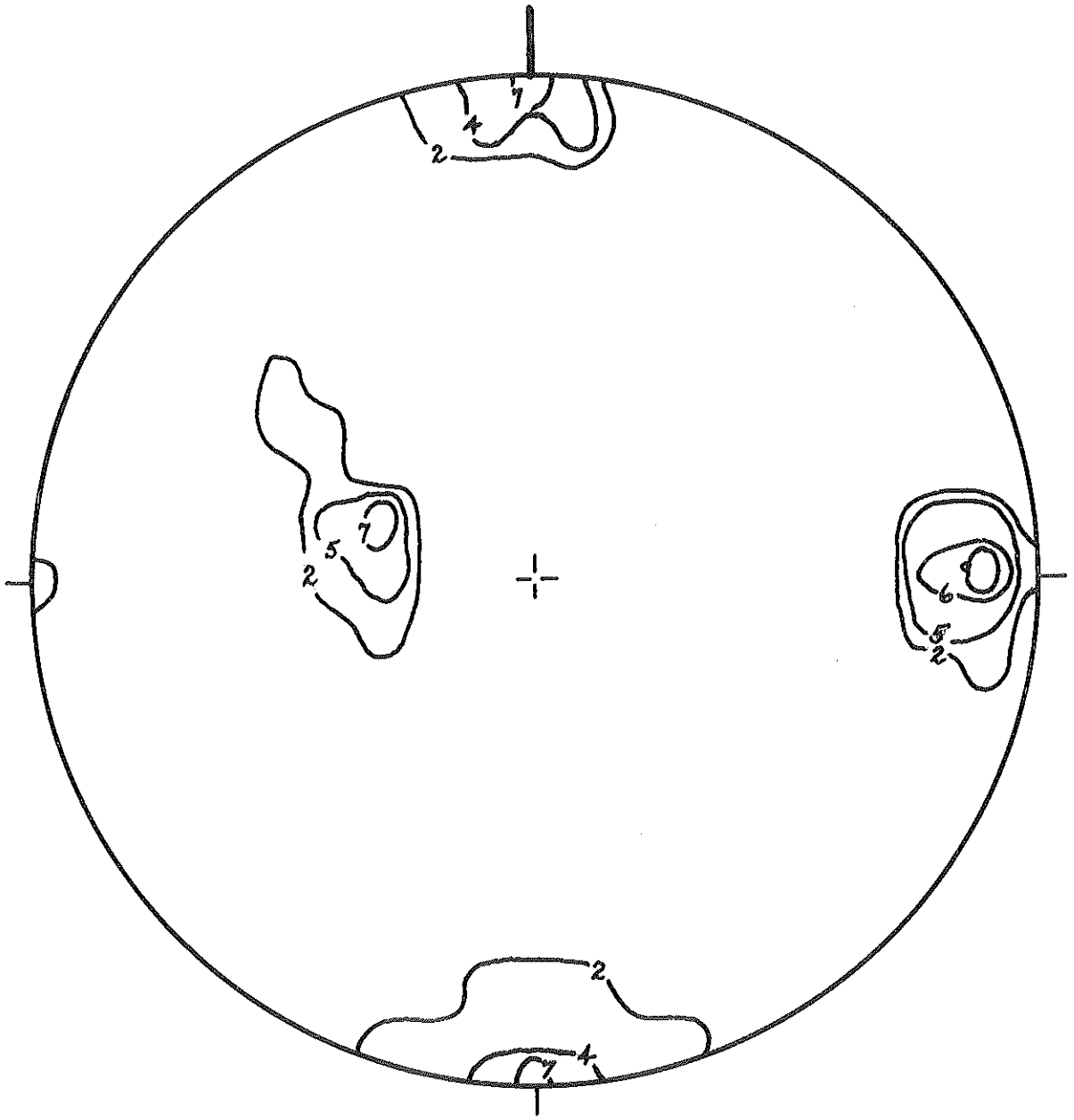

Fig. 3 (S) Contour drawing of equal area plot of poles to joints in a rock mass.

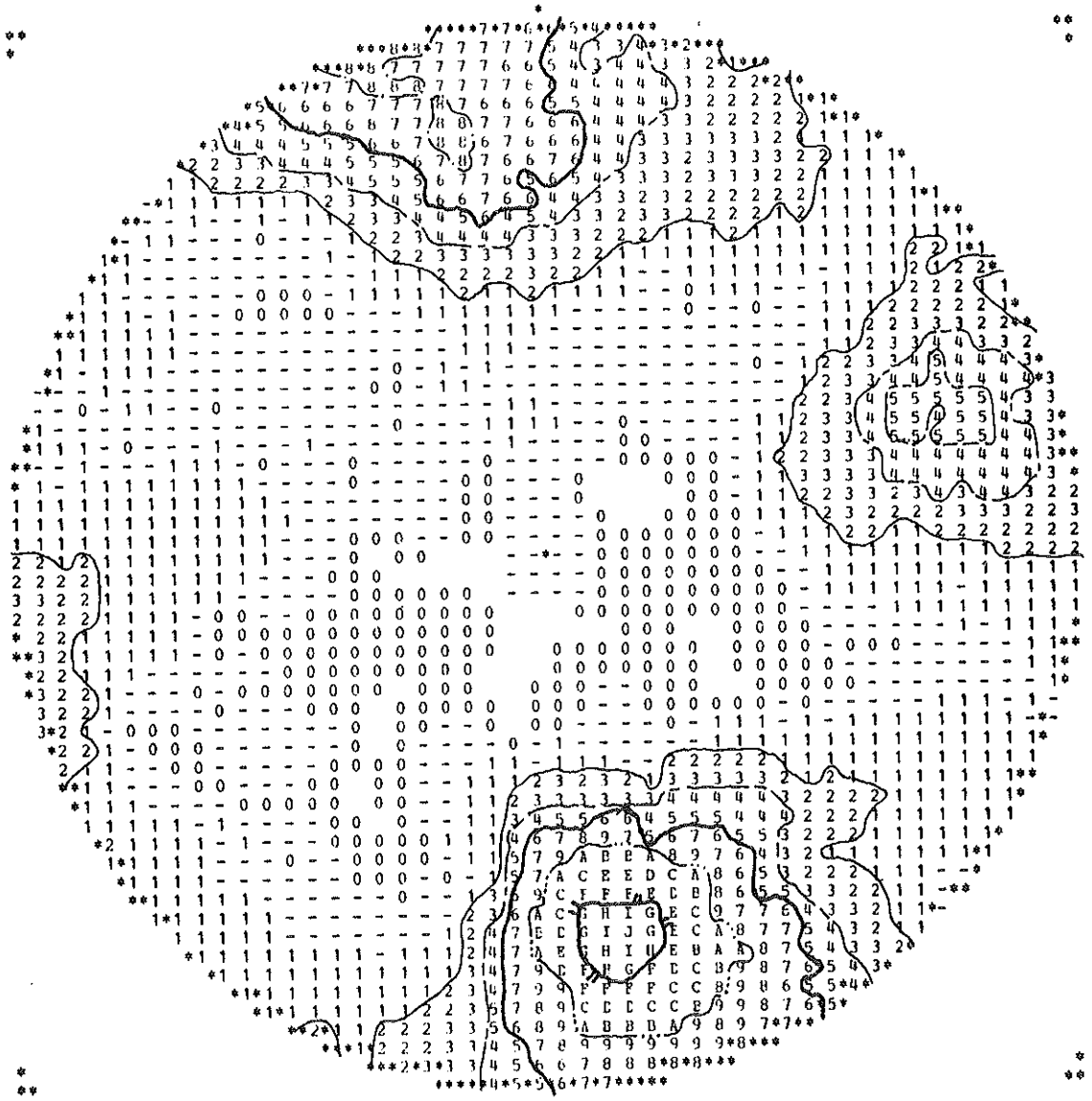

Fig. 4 (S)(a) Contoured equal angle stereographic projection of joints in a rock mass. 565 (obs)

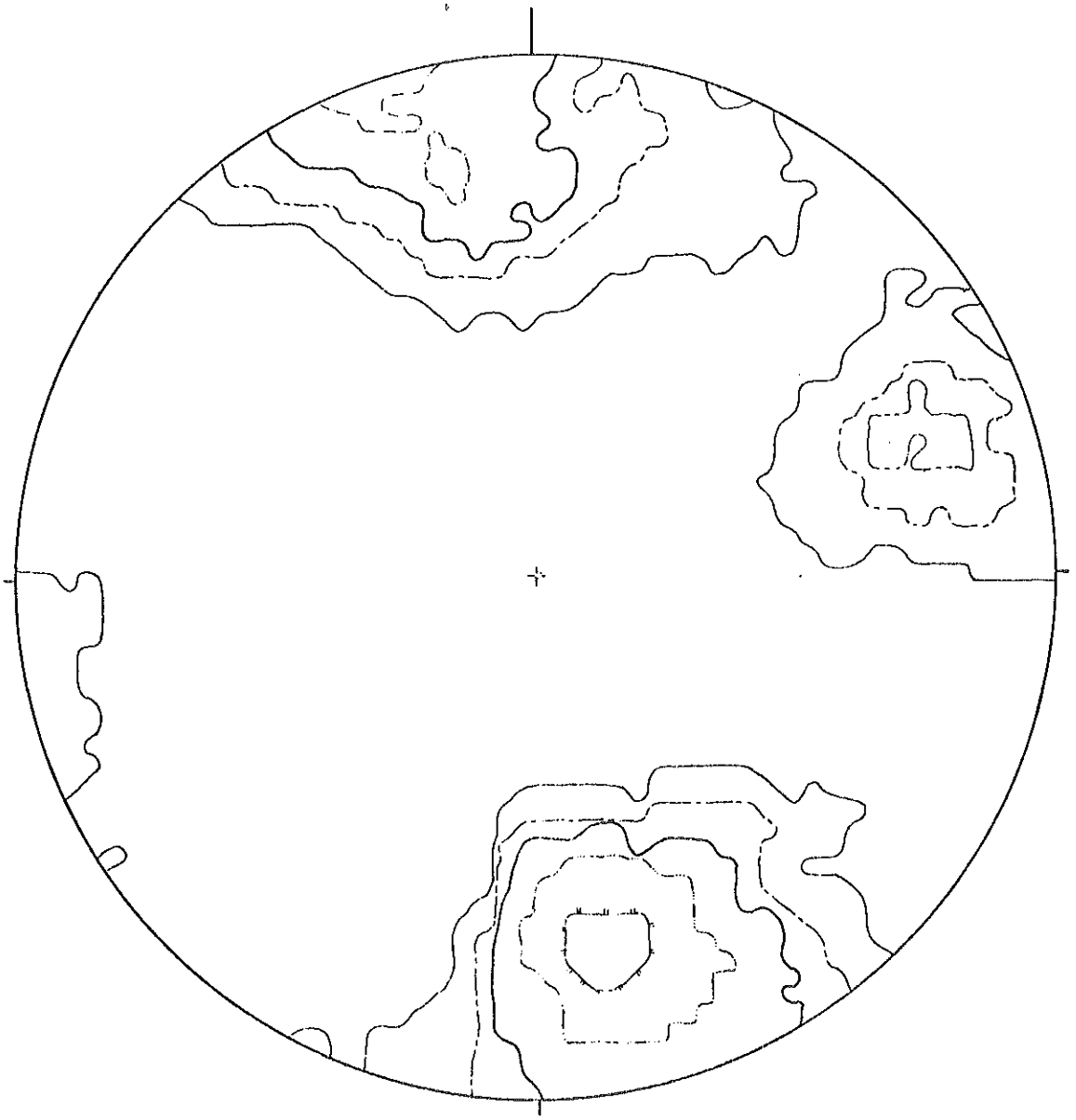

Fig. 4 (S)(b) Contoured equal angle stereographic projection of joints in a rock mass. 565 (obs)

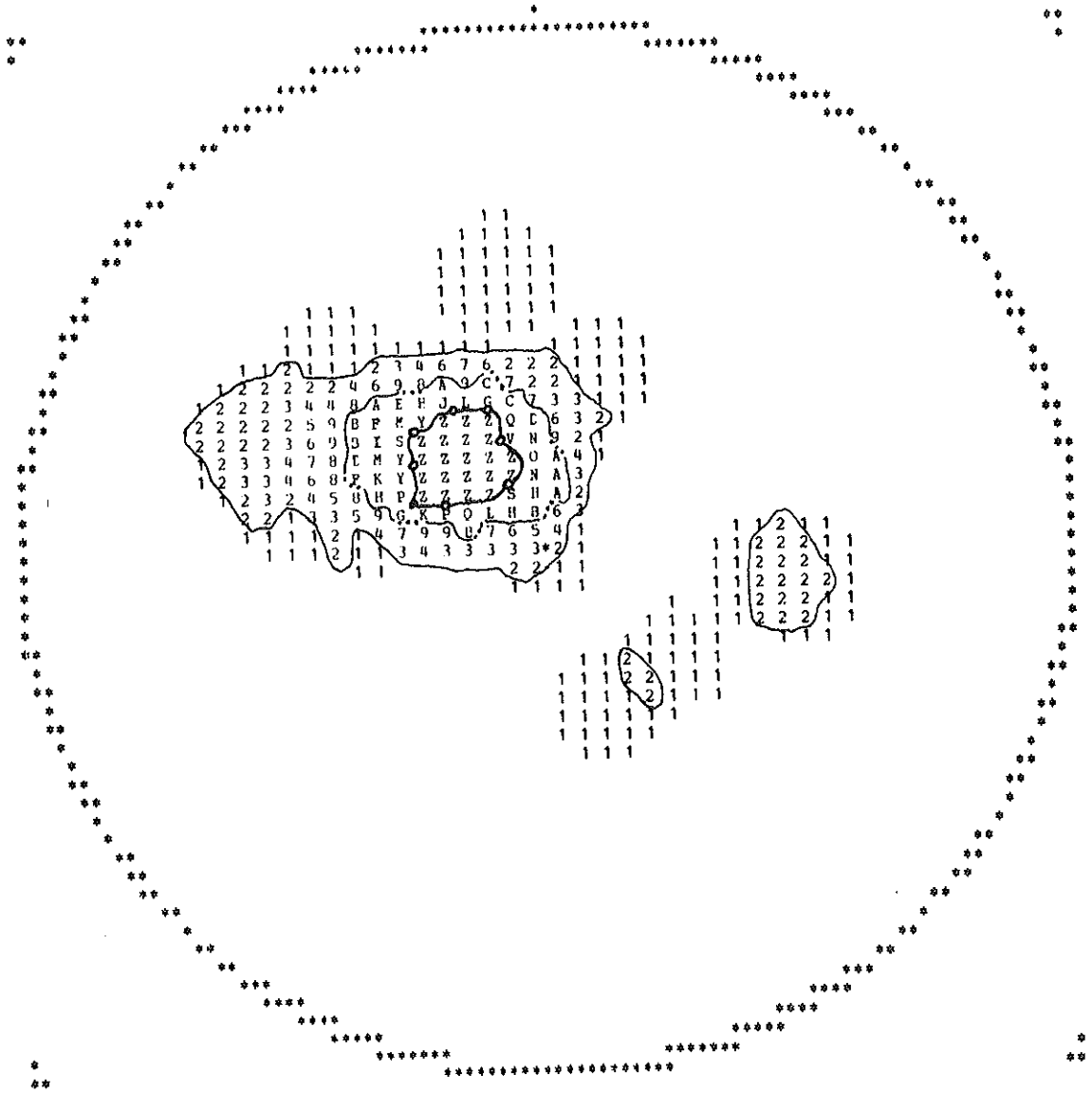

Fig. 5 (S)(a) Contoured equal angle stereographic projection of bedding in a rock mass. (97 obs)

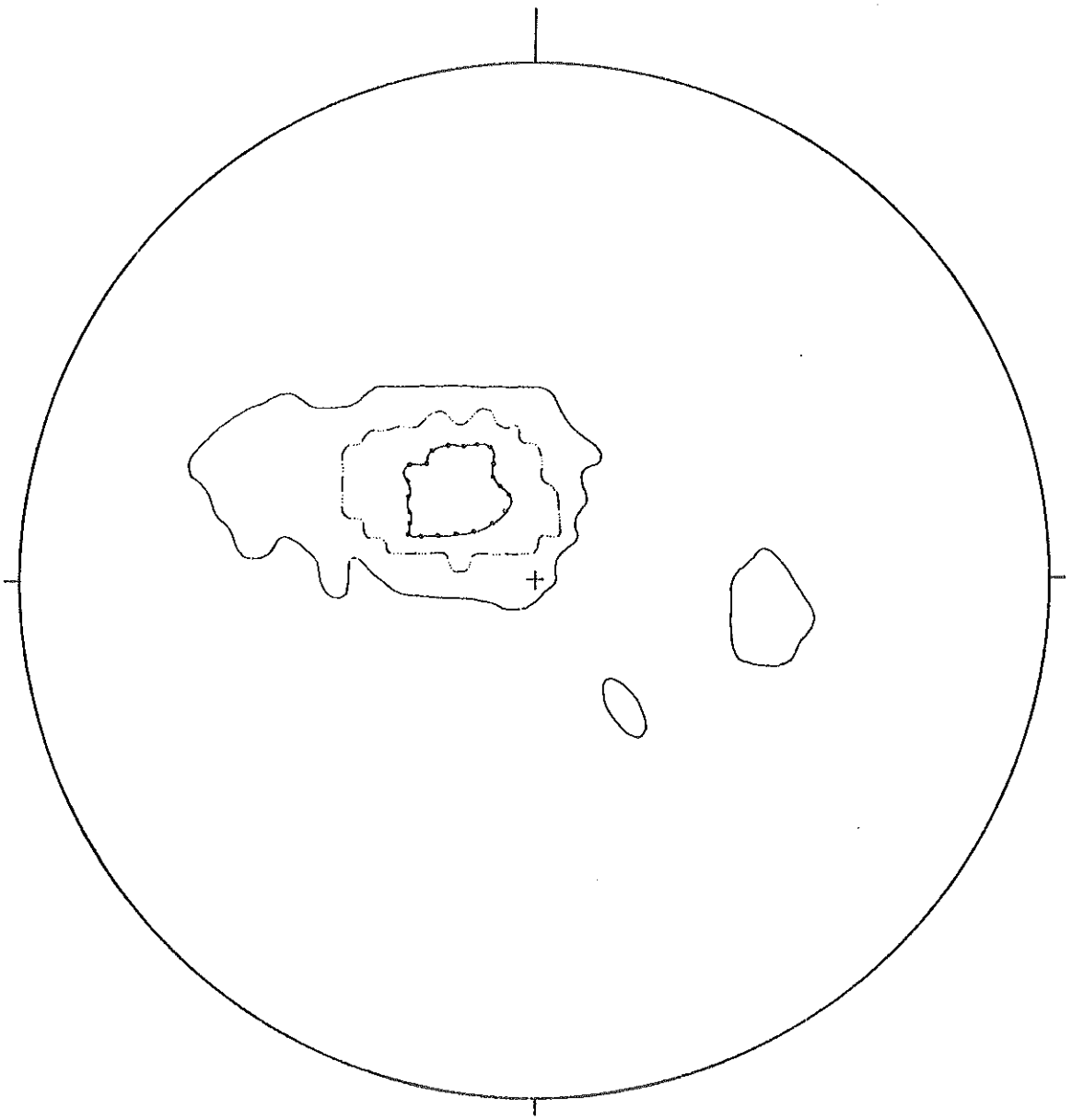

Fig. 5 (S)(b) Contoured equal angle stereographic projection of bedding in a rock mass (97 obs).

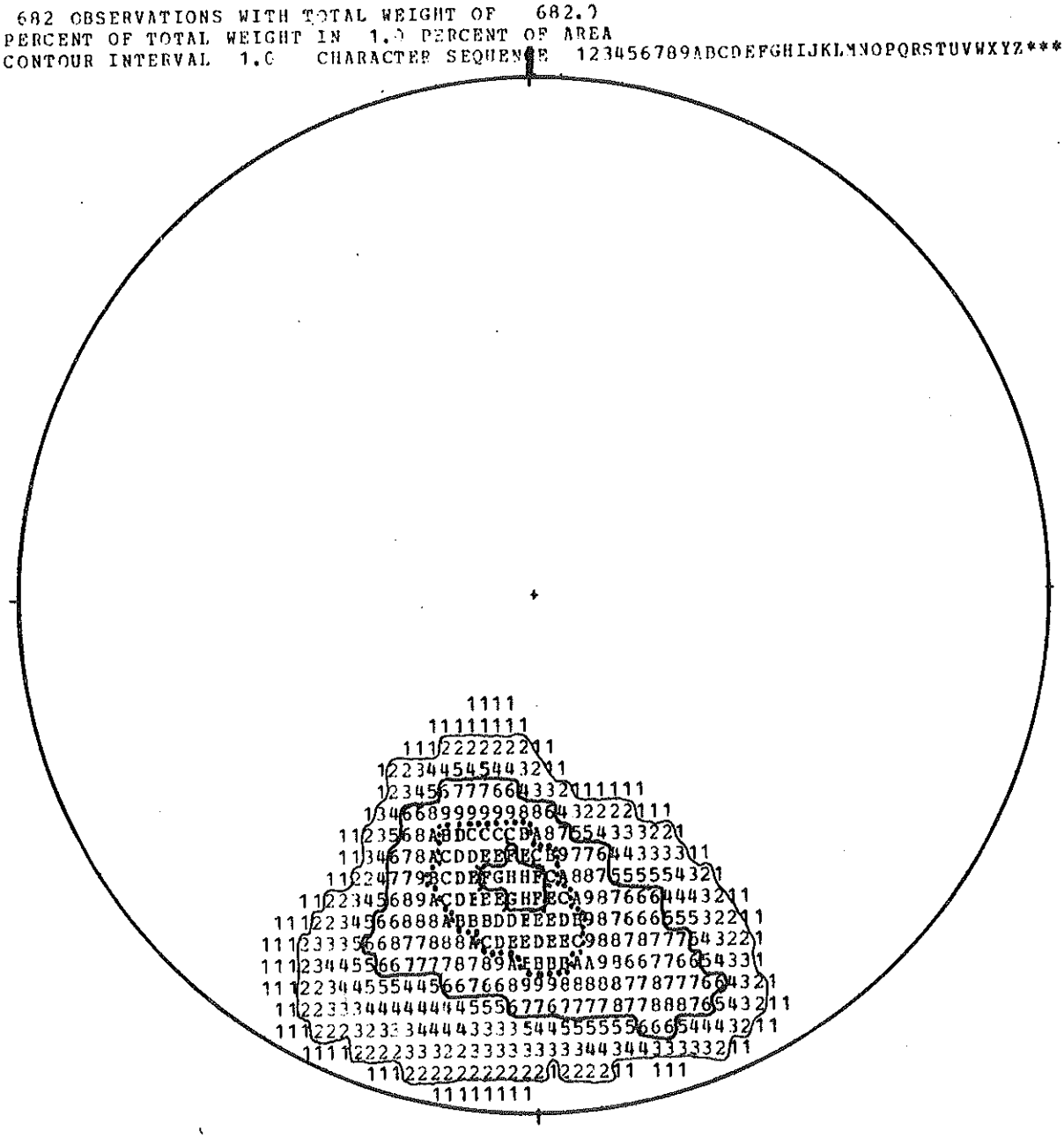

Fig. 7 (S) Contoured equal area projection of foliation joints in a rock mass (682 obs).

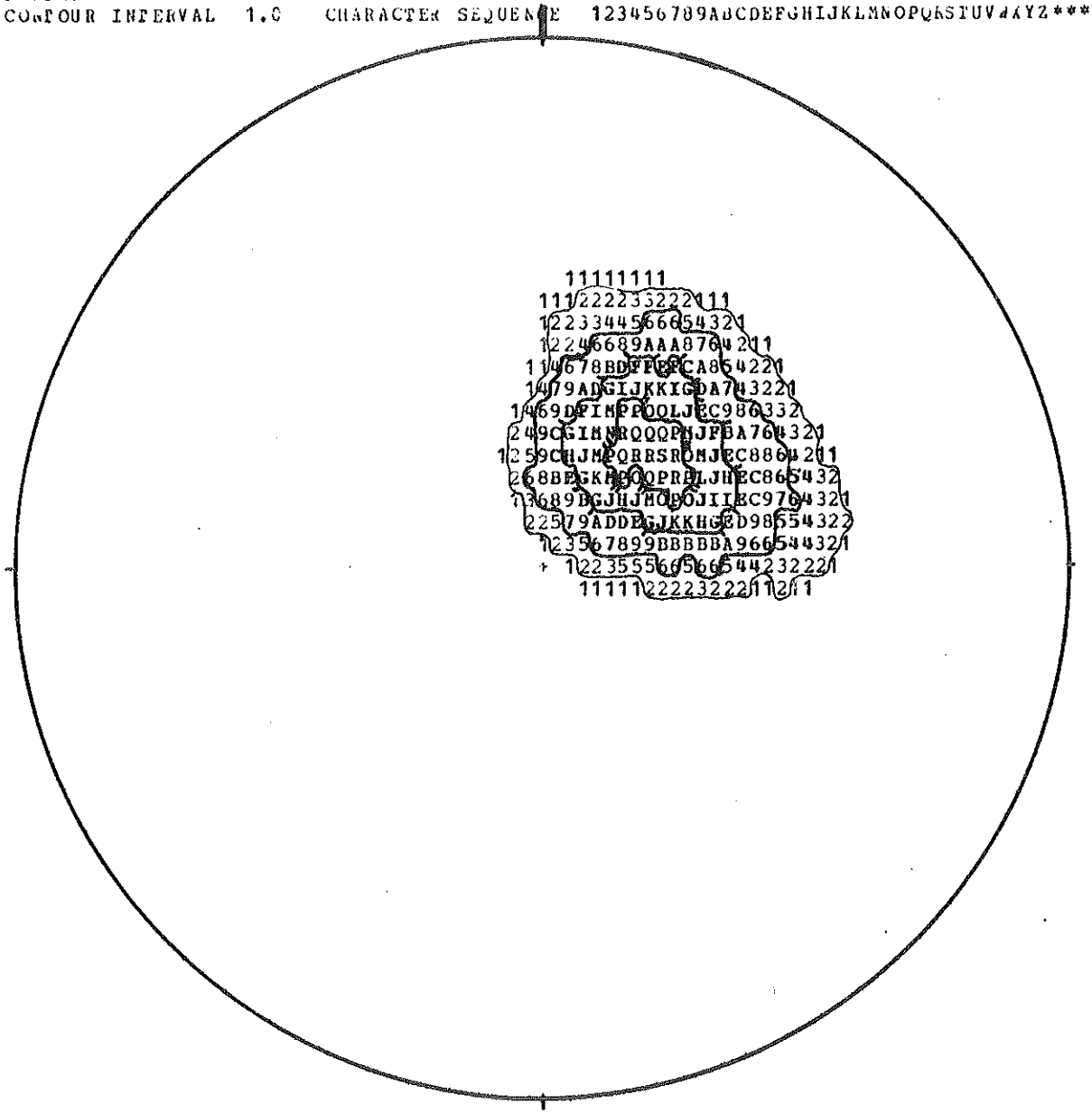

Fig. 8 (S) Contoured equal area projection of a joint set in a rock mass (440 obs).